PET/CT imaging of 3D printed devices in the gastrointestinal tract of rodents

Alvaro Goyanes[1*], Anxo Fernández-Ferreiro[2,*], Adil Majeed[3], Noemí Gomez-Lado[4], Atheer Awad[3], Andrea Luaces-Rodríguez[2], Simon Gaisford[1,3], Pablo Aguiar[4,†] , Abdul W. Basit[1,3,†]

[1]FabRx Ltd., 3 Romney Road, Ashford, Kent, TN24 0RW, UK.

[2]Pharmacy Department. Clinical Pharmacology Group. University Clinical Hospital, Health Research Institute of Santiago de Compostela (IDIS)(SERGAS). Spain.

[3]UCL School of Pharmacy, University College London, 29-39 Brunswick Square, London, WC1N 1AX, UK.

[4]Molecular Imaging Group, Faculty of Medicine, USC, University Clinical Hospital, Health Research Institute of Santiago de Compostela (IDIS). Spain.

* Equally contributed

† Co-corresponding authors

Corresponding authors:

Abdul Basit

a.basit@ucl.ac.uk

Pablo Aguiar

pablo.aguiar.fernandez@sergas.es

Keywords:

Additive manufacturing, Three dimensional printing; fused deposition modeling; positron emission tomography; computed tomography, Printlets^{TM}.

Abstract

Fused deposition modelling (FDM) 3D printing (3DP) is a revolutionary technology with the potential to transform drug product design in both the pre-clinical and clinical arena. The objective of this pilot study was to explore the intestinal behaviour of four different polymer-based devices fabricated using FDM 3DP technology in rats. Small capsular devices of 8.6mm in length and 2.65mm in diameter were printed from polyvinyl alcohol-polyethylene glycol graft-copolymer (PVA-PEG copolymer, Kollicoat IR), hydroxypropylcellulose (HPC, Klucel), ethylcellulose (EC, Aqualon N7) and hypromellose acetate succinate (HPMCAS, Aquasolve-LG). A smaller sized device, 3.2mm in length and 2.65mm in diameter, was also prepared with HPMCAS to evaluate the cut off size of gastric emptying of solid formulations in rats. The devices were radiolabelled with Fluorodeoxyglucose (^{18}F-FDG) and small animal positron emission tomography/computed tomography (microPET/CT) was used to track the movement and disintegration of the fabricated devices in the rats. The PVA-PEG copolymer and HPC devices disintegrated after 60min following oral administration. The EC structures did not disintegrate in the gastrointestinal tracts of the rats, whereas the HPMCAS-based systems disintegrated after 420min. Interestingly, it was noted that the devices which remained intact over the course of the study had not emptied from the stomach of the rats. This was also the case with the smaller sized device. In summary, we report for the first time, the use of a microPET/CT imaging technique to evaluate the *in vivo* behaviour of 3D printed formulations. The manipulation of the 3D printed device design could be used to fabricate dosage forms of varying sizes and geometries with better gastric emptying characteristics suitable for rodent administration. The increased understanding of the capabilities of 3DP in dosage form design could, henceforth, accelerate pre-clinical testing of new drug candidates in animal models.

1. Introduction

Three-dimensional printing (3DP) has the potential to revolutionise the future design and manufacture of medicines. With this technology, personalised doses to specific individuals is a promising objective (Sanderson 2015). Therefore, 3DP may shift the scope of manufacture from mass-produced restricted dose-range unit forms in the pharmaceutical industry to on-demand production of patient-specific medicines, integrated in pharmacies or hospitals (Alomari et al. 2015). Moreover, the ability of 3DP to readily prepare formulations with different dose strengths may facilitate pre-clinical studies in animals. This could be used to determine a range of safe doses for first-in-man studies and to assess the safety profile of new active compounds.

3DP can be used to produce 3D printed solid dosage forms (Printlets^{TM}) in a repeatable and efficient manner, with the capability to combine multiple drugs in one formulation (Goyanes et al. 2015c, Khaled et al. 2015b). With the application of intelligent design features (Markl et al. 2017), 3DP formulations can exhibit immediate or modified release characteristics, or even combinations of these (Goyanes et al. 2015b, Goyanes et al. 2014, Goyanes et al. 2017, Okwuosa et al. 2017). There are various types of 3DP technologies commercially available for pharmaceutical use, namely from stereolithography (Wang et al. 2016), selective laser sintering (Fina et al. 2017), and material extrusion, for example (Khaled et al. 2015a). However, fused-deposition modelling (FDM) remains the most affordable, easy to operate and most versatile method of manufacture for unit-dose fabrication (Goyanes et al. 2015a). In FDM, an extruded filament is passed through a heated nozzle, utilised to soften the polymer filament. This allows the formulation to be deposited layer by layer onto the build plate of the printer in x-y dimensions to produce the required design. It is possible to obtain several drug release profiles from Printlets^{TM} by altering the parameters of the 3DP software, such as the infill, layer thickness (Goyanes et al. 2016) or through excipient selection (Goyanes et al. 2017, Melocchi et al. 2015, Melocchi et al. 2016, Okwuosa et al. 2017).

The use of molecular imaging technologies has optimised the development and evaluation of drug delivery systems (Fernandez-Ferreiro et al. 2017, Ding and Wu 2012). These technologies involve non-invasive procedures which significantly decrease the number of animals used for analysis whilst increasing the number of measurements taken for each animal (Cunha et al. 2014, Capozzi et al. 2013). Techniques such as magnetic resonance imaging (MRI) (Schiller et al. 2005) and scintigraphy (Tuleu et al. 2007, Weinstein et al. 2013) have been applied to pharmacokinetic studies for orally-administered dosage forms.

Morphological techniques such as computed tomography (CT), for example, have also been used for the tracing of capsules along the gastrointestinal (GI) tract (Saphier et al. 2010). Unlike other medical imaging techniques, CT enables the direct imaging and differentiation of soft tissue structures. In addition, due to short scanning times of approximately 500 milliseconds to a few seconds, CT can be used for all anatomic regions, including those susceptible to motion and breathing. Positron emission tomography (PET) is a further example of a functional imaging technique used for pharmacokinetic studies of oral dosage forms (Shingaki et al. 2012). PET allows for a three dimensional mapping of positron emitting radiopharmaceuticals to detect blood flow, glucose metabolism and receptor densities in biological tissues (Lameka, Farwell and Ichise 2016). The use of integrated information from PET and CT technologies enable radiopharmaceutical release data to be obtained in combination with the anatomical position of the formulation at different times, and thus, creates a powerful imaging tool (Anand, Singh and Dash 2009).

As rodents are often used in the pre-clinical arena (Hatton et al. 2015), the aim of this pilot study was to investigate the in vivo behaviour of four different FDM 3D printed structures in rats. Printed devices with different release characteristics, dependent on polymer composition, were fabricated. This included a polyvinyl alcohol/polyethylene glycol graft copolymer (PVA-PEG graft-copolymer, immediate release), hydroxypropylcellulose (HPC, non-ionic water-soluble), ethylcellulose (EC, non-soluble sustained release) and hydroxypropyl methylcellulose acetate succinate LG (HPMCAS, pH dependent). The capsular devices were prepared with different lengths (2.65mm diameter x 8.6mm length and 2.65 mm diameter x 3.2 mm length) to evaluate the cut off size of gastric emptying of solid dosage forms in rats. The selected shell was designed to be 0.5mm thick in order to develop formulations that were more resistant to the contractions of the GI tract. In addition, the shell would provide a more reliable drug release profile of the different regions of the GI tract. These 3DP devices were characterised by microPET/CT in order to evaluate their *in vivo* performance in rats. To the authors' knowledge, there are currently no previous examples of *in vivo* studies regarding FDM 3D printed formulations using rodent models. Therefore, the work reported is the first study of its kind to evaluate the feasibility of using fused microPET/CT technologies as a method of investigating the passage and disintegration of novel FDM 3D printed devices.

2. Materials and methods

Materials

Fluorodeoxyglucose (^{18}F-FDG) TRACERlab MX synthesizer (GE Healthcare®) was used as a tracer.

Four types of polymers were investigated as the main excipient: polyvinyl alcohol/polyethylene glycol graft copolymer – PVA/PEG (Kollicoat® IR, an immediate release polymer) was obtained from BASF, Germany; hydroxypropylcellulose - HPC (Klucel® EF, a non-ionic water soluble polymer), ethylcellulose – EC (Aqualon® N7, a non-soluble polymer) and hydroxypropylmethylcellulose acetate succinate - HPMCAS LG (Aquasolve®-LG, a pH dependent polymer with a pH threshold of 5.5 (Rowe, Sheskey and Quinn 2009)) were obtained from Ashland, UK. D-Mannitol (Sigma-Aldrich, UK) and methylparaben NF grade (Amresco, USA) were used as a plasticizer. Magnesium stearate and Talc (Sigma-Aldrich, UK) were used as lubricants.

AquaCem® a light-yellow, translucent glass-ionomer luting material consisting of a blend of alumino-silicate glass and polyacrylic acid was used as a cement to seal the devices (Dentsply, UK.).

Methods

Preparation of filaments by hot melt extrusion (HME)

Filaments of different polymers were prepared via hot melt extrusion. The appropriate excipients were weighed and mixed using a pestle and mortar to produce a uniform powder of 40g in weight (Table 1). The mixture was then extruded using a single-screw filament extruder (Noztec Pro hot melt extruder, Noztec, UK) in order to obtain the filament (extrusion temperature 105-145°C, Table 1, nozzle diameter 1.75mm, screw speed 15rpm). The extruded filaments were protected from light and kept in a vacuum desiccator until printing.

Table 1. Composition of the filaments produced via HME

Formulation	Kollicoat IR (%)	Klucel EF (%)	Aqualon N7 (%)	Aquasolve LG (%)	Methylparaben (%)	Mannitol (%)	Talc (%)
Kollicoat IR	45	-		-	20	20	10
Klucel EF	-	73.75		-	-	21.25	
Aqualon N7			75		20		
Aquasolve-LG	-	-		70	15	-	10

*5% Magnesium Stearate was used in all the formulations as a lubricant

3D Printing of the devices

Devices were fabricated from the extruded filaments using a standard MakerBot Replicator 2X Desktop 3D Printer (MakerBot Inc., USA). The templates used to print the devices were designed with 123D Design Software (Autodesk Inc., USA) and exported as a stereolithography file (.stl) into the 3D printer software (MakerWare v. 2.4.1, MakerBot Inc., USA).

The device design selected (8.6mm length x 2.65mm diameter, shell thickness of 0.5mm, Figure 1) is an adaptation from a size 9 capsule used for dosing of small rodents. Smaller capsular devices with a length of 3.2 mm x 2.65mm diameter were also prepared.

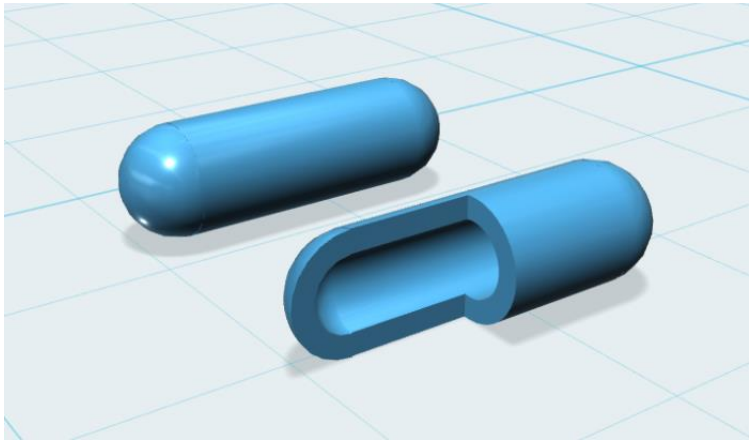

Figure 1. 3D representation of the capsular device (8.6mm length x 2.65mm diameter - 0.5mm shell thickness), cross section (front) and complete (back)

The printer settings were as follows: the infill percentage of the shell was 100%, a high resolution with the raft option was activated and, the speed whilst extruding was 3mm/s, the speed while traveling was 25mm/s, the z-axis travel speed was at 23mm/s, the number of

shells was 2 and the layer height set at 0.10mm. Printing temperatures were modified depending on the type of filaments used to print the device (Table 2).

Table 2. Printing settings for the filaments

Formulation	Printing Temperature (°C)	Platform Temperature (°C)
Kollicoat IR	155	40
Klucel EF	160	0
Aqualon N7	160	0
Aquasolve LG	175	0

X-ray Micro Computed Tomography (Micro-CT)

A high-resolution X-ray micro computed tomography scanner (SkyScan1172, Bruker-microCT, Belgium) was used to 3D visualize the structure of the 3D printed devices. Samples were scanned without the use of a filter at a resolution of 2000x1048 pixels. Image reconstruction was performed using NRecon software (version 1.7.0.4, Bruker-microCT). Beam hardening, ring artefacts and post alignments were adjusted to achieve the best possible images. 3D model rendering and viewing were performed using the associate program CT-Volume (CTVol version 2.3.2.0) software. The collected data was analysed using the software CTVox (CTVox version 3.2).

Device morphology characterisation

Pictures of the devices were taken with a Nikon CoolpixS6150 with the macro option activated.

In vivo microPET/CT studies

Once printed, the devices were cut 1mm from the end using a scalpel and filled with approximately 5µL of ^{18}F-FDG with an activity of 3MBq using a HPLC syringe. The dental cement (AquaCem®) was used to close the devices. One spatula of adhesive powder (approx. 100mg) was mixed with two drops of water (approx. 30mg) to prepare the adhesive paste. The paste was applied using a small spatula onto the removed portions of the devices that were reattached to the larger section in less than 2min after mixing of the adhesive. Once applied, the devices were allowed to dry for 10min for the solidification of the adhesive.

This study was carried out on male Sprague-Dawley rats with an average weight of 300g supplied by the animal facility at the University of Santiago Compostela (USC). During the experiment, the animals were kept in individual cages with free access to food and water in a room under controlled temperature (22±1ºC) and humidity (60±5%) conditions and with day-night cycles regulated by artificial light (12/12h). For the administration of the 3D printed devices, the animals were placed in a gas chamber containing 2% isoflurane in oxygen to induce anaesthesia. The radiolabelled devices were introduced directly into the stomach of the rats using a Torpac® dosing syringe for rodents. Four rats were used for testing each type of device.

MicroPET/CT acquisition

PET/CT images were acquired using an Albira microPET/CT Preclinical Imaging System (Bruker Biospin, Woodbridge, Connecticut, United States). The PET subsystem comprises three rings of eight compact modules based on monolithic crystals coupled to multi-anode photomultiplier tubes (MAPMTs), forming an octagon with an axial FOV of 40mm per ring and a transaxial FOV of 80mm in diameter. The computed tomography (CT) system comprises a microfocus x-ray tube and a CsI scintillator 2D pixelated flat panel detector. Immediately after the administration of the device, the animals were positioned onto the bed of the scanner to allow dynamic PET acquisitions at predetermined time intervals. Rats remained conscious for most of the experiment and only were anesthetized during PET/CT acquisition. No contrast or prokinetic agents were administered to the rats.

PET/CT image analysis

Firstly, device disintegration was assessed by visual inspection of the spread of the tracer. Furthermore, CT images were obtained for evaluation of the gastric retention and fused PET/CT images were used to track the devices along the gastrointestinal tract. Quantitative analysis was carried out by using Regions of Interest (ROIs) manually delineated on the position of the device. This was obtained from the first PET image frame and overlapped on subsequent image frames. The average activity of the radiotracer in the device was gathered over time. The effect of the radioactive decay was calculated (110min halftime for ^{18}F-FDG) and removed from the measurements. Results are presented as the % of radioactivity remaining in the device over time.

Results and Discussion

Four types of 3D printed devices were fabricated with filaments obtained by hot melt extrusion (HME) using four base polymers, namely an immediate-release polymer (Kollicoat

IR, PVA-PEG copolymer), a non-ionic water-soluble polymer (Klucel EF, HPC), an insoluble polymer (Aqualon N7, EC) and a pH dependent polymer with a pH threshold of 5.5 (Aquasolve-LG, HPMC-AS LG) (Figure 2).

Figure 2. From left to right pictures of 3D printed devices of Kollicoat IR, Klucel EF, Aqualon N7 and Aquasolve-LG (units are cm).

These polymers were selected based on their different dissolution characteristics. Alongside the chosen polymer, the filaments further incorporated a plasticiser (methylparaben or mannitol) and a lubricant (talc or magnesium stearate) (Table 1). The inclusion of plasticisers and lubricants in the correct ratios was crucial to obtain filaments that would have the required properties for printing capsular devices of such small a size. In a previous study (Melocchi et al. 2016), disks fabricated by FDM printing with similar types of polymers were used as a simple model to evaluate the performance of printed barriers when in contact with aqueous fluids using an *in vitro* test cell assembly. It was found that the optimisation of the formulation with the use of plasticisers and lubricants was required to enhance the printability of these filaments, and thus, refined the printing characteristics of smaller objects. The optimal printing temperature and settings were determined and are outlined in the printing results (Table 2).

MicroCT images revealed that all fabricated devices were not compromised and showed no visible holes in the surface of the shells (Figure 3). The Aquasolve-LG devices appeared to be less uniform in its deposition, however, exhibiting a more deformed shape. Visual analysis of the Aquasolve-LG device showed a slight reduction in its volume when compared with the other FDM printed devices.

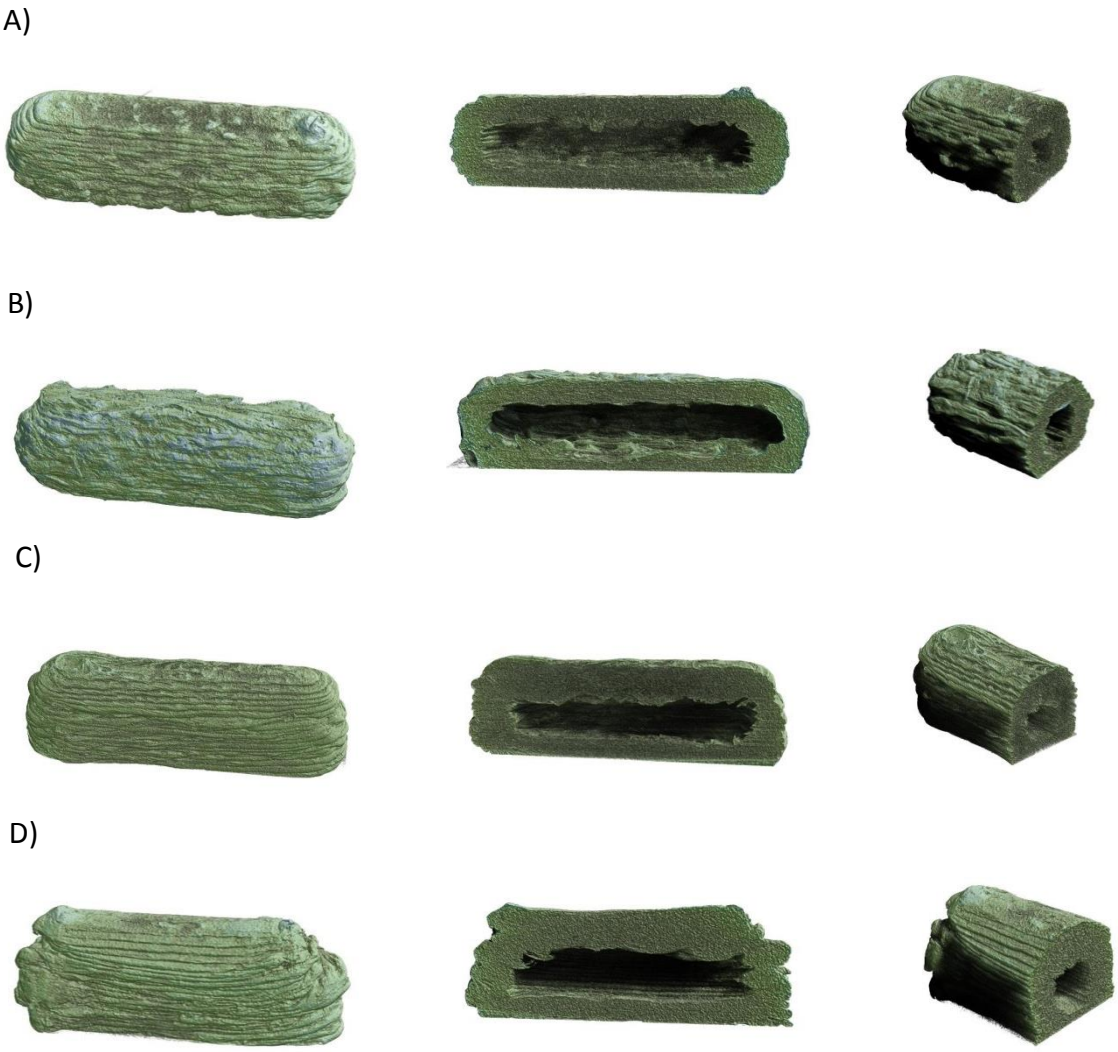

Figure 3. Micro-CT images of 3D printed devices made of: A) Kollicoat IR, B) Klucel EF, C) Aqualon N7 and D) Aquasolve-LG

In order to evaluate their release properties, the 3D printed devices were cut and reassembled following the introduction of the ^{18}F-FDG marker. It might have been possible to load the tracer into the capsular devices using a dual FDM 3D printer with two filaments; one for the external shell and other for the core (Markl et al. 2017, Okwuosa et al. 2017, Goyanes et al. 2015c). However, in our study, we followed a manual approach for two reasons; firstly, to avoid the contamination of the printers with the radiotracer and; secondly, due to the short half-life of ^{18}F-FDG. This was necessary as the printing process and the PET study were performed at different institutions. It has been reported that it is possible to print the body and cap of a capsule separately and then join them together after filling (capsule size 11.95mm length x 8mm diameter) (Melocchi et al. 2015). However, this

approach was not feasible with the current study due to the small size of the devices needed for administration to rodents.

The devices were placed into the stomach of the rats and the behaviour of the devices within the GI tract were evaluated by PET/CT imaging. The results indicated that the disintegration of the devices were identified at different times following oral administration in rats, although this was dependent on the type of device (Figure 4).

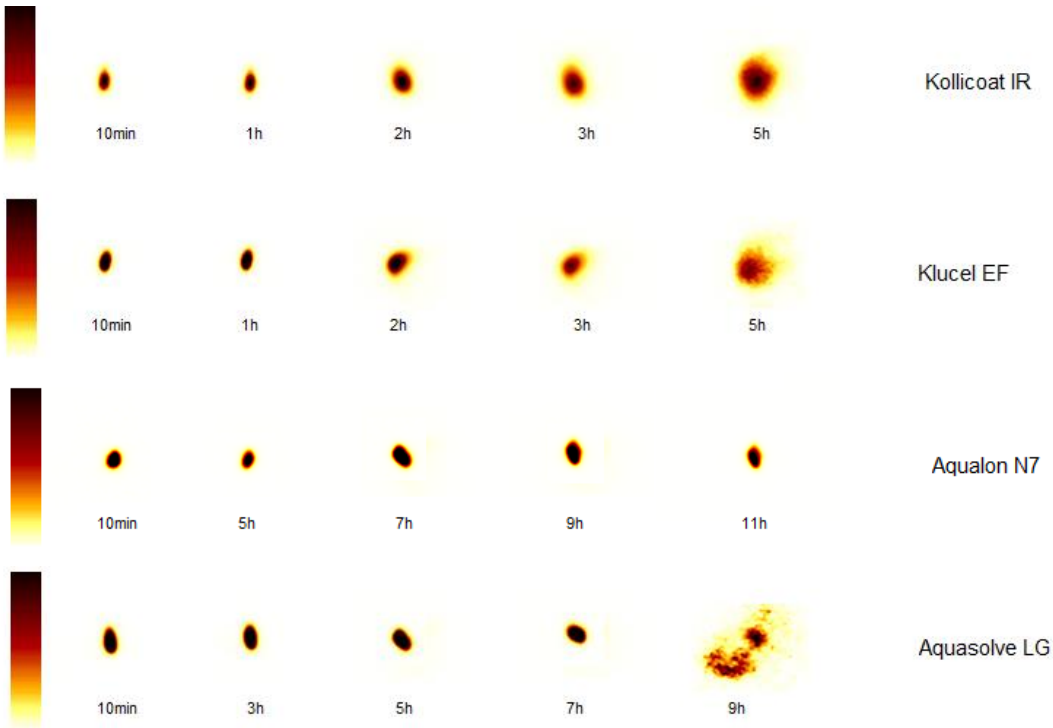

Figure 4. Coronal views of PET images after oral administration of radiolabelled Kollicoat IR, Klucel EF, Aqualon N7 and Aquasolve-LG devices. The black hue indicates high levels of radioactivity.

The combination of PET and CT technologies allowed the location of the device in the GI tract to be visualised. The *in vivo* disintegration of the Kollicoat and Klucel devices demonstrated similar release behaviours, occurring in the stomach between 60min and 120min after administration (Figure 5). Kollicoat IR is a pharmaceutical excipient that was specifically designed to manufacture instant release tablets (Janssens et al. 2007). The thickness of the device (approximately 0.5mm), however, is much thicker than the regular polymeric coatings of tablets (in the range of 20-100µm (Liu et al. 2009), therefore delaying device disintegration

.

Aqualon-based devices remained unchanged and did not exhibit any signs of disintegration after 11 hours. Although the polymer is not soluble, Aqualon is normally incorporated to manufacture sustained release tablets where the drug dissolution rate is controlled by drug diffusion through the coating of the tablet. In this case, the diffusion of tracer was not observed through the wall of the capsular device, indicating that the wall was too thick. It has been established that drug release is dependent on barrier thickness (Melocchi et al. 2016, Okwuosa et al. 2017) and therefore, the preparation of devices with thinner walls could represent a strategy to achieve the release of the tracer from the devices over time. Finally, the disintegration of Aquasolve was clearly delayed, showing a disintegration time between 420 to 540min.

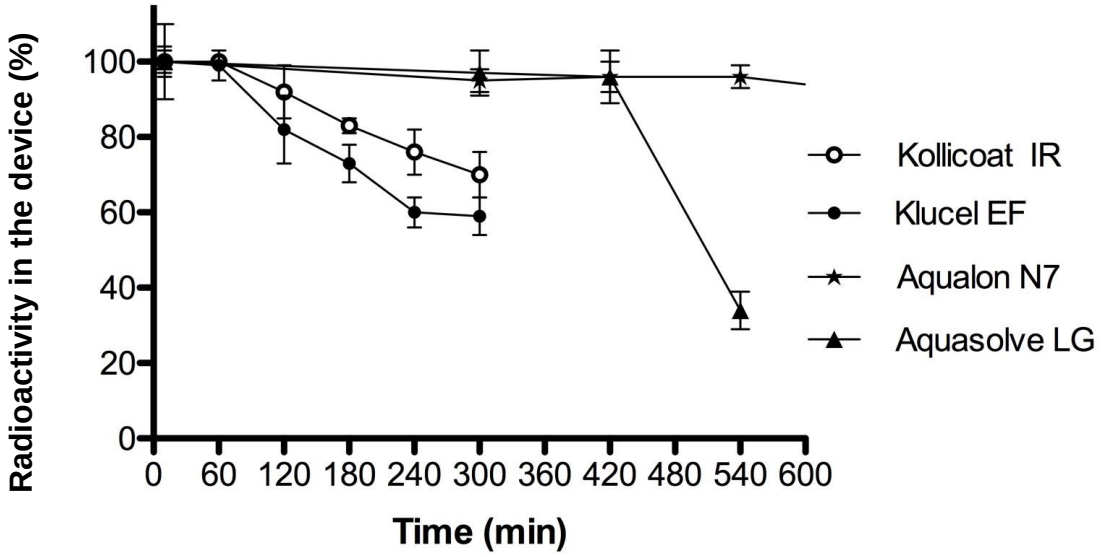

Figure 5. Dynamic study of disintegration behaviour of the four capsular devices (n=4).

Fused PET/CT images taken after the administration of Kollicoat, Klucel, Aqualon and Aquasolve devices showed that all the devices were retained in the stomach without passing to the small intestine prior to disintegration. As an example, Figure 6 shows the fused PET/CT images after administration of the Klucel-based device.

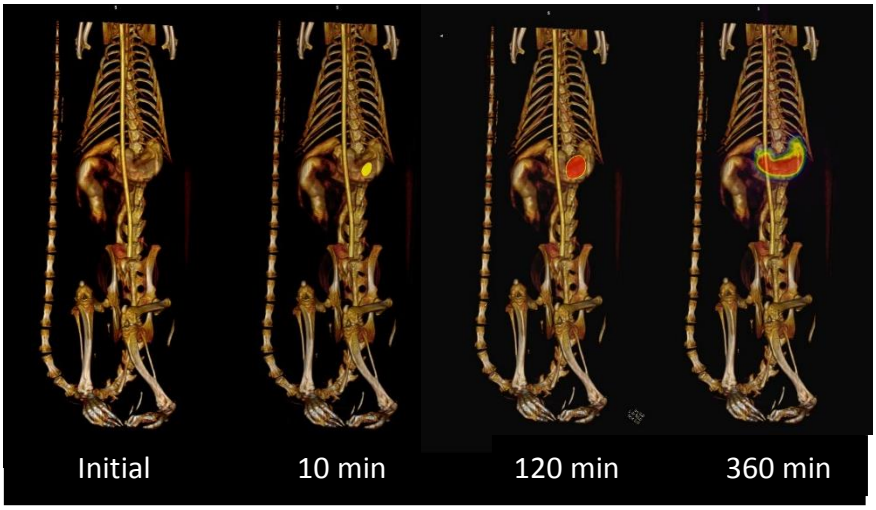

Figure 6. Fused image PET/CT. a) Prior to the administration of the Klucel device b) 10min c) 120min and d) 360min post-administration.

The long disintegration lag time of Aquasolve (more than 420 minutes) could be explained by the fact that the devices did not empty the stomach. Aquasolve-LG is known to dissolve at pH 5.5, however, the gastric pH of the rat is between 3 and 5 (Hatton et al. 2015, McConnell, Basit and Murdan 2008), and thus, provides a rationale for its retarded dissolution. A possible explanation for the lack of gastric emptying in rats might be related to the size of the dosage form. The study was repeated with smaller Aquasolve devices with a length of 3.2mm (compared with the standard 8.6mm length of x 2.65mm diameter). After administration of these smaller devices to the rats, however, the results surprisingly showed that none of these formulations emptied from the stomach either.

The gastric emptying or retention of orally-administered dosage forms in rodent models are currently poorly understood and are subject to varying parameters such as: gastric mobility (Dalziel et al. 2017), size of dosage form (Dalziel et al. 2016), the effect of anaesthesia (Yamashita et al. 2011) and potentially pre- or post-prandial states (Mori 1989), to name a few. A study, for example, demonstrated that enteric-coated gelatine size 9 capsules were able to empty from the stomach of a rat between 2 to 8h after administration (Albrecht et al. 2006). With the use of single-PET/CT x-ray technology, another study demonstrated that enteric-coated capsules emptied from the stomach and liberated the nanoparticle contents in the proximal region of the small intestine (Sonaje et al. 2010). In other studies, enteric coated capsules were reported to be released in the lower GI tract (Hatch et al. 2006, Shah, Nutan and Khan 2004, Oveisi et al. 2004). Despite a number of studies suggesting that size 9 coated capsules do empty from the stomach, contention still remains to whether these devices are the optimum dimensions or geometries. A study showed that only capsules up

to 3.5mm in diameter and 4.8mm in length are able to do so (Saphier et al. 2010). In the same study, capsules emptied more rapidly from fed stomachs when compared with fasted rats. This finding was unexpected as food is generally considered to delay gastric emptying (Varum, Hatton and Basit 2013). Therefore, a better understanding of gastric emptying and retention can be explored through 3DP due to its capabilities of fabricating varying shapes and sizes, which can also manipulate drug release characteristics (Goyanes et al. 2015c).

3. Conclusions

This is the first study to demonstrate the viability of FDM 3DP as a meaningful and feasible method of manufacturing of small capsular devices, as evaluated *in vivo* studies with the utilisation of microPET/CT imaging. The devices were successfully 3D printed using four different polymer filaments: Kollicoat IR (immediate release), Klucel EF (water soluble), Aqualon N7 (insoluble polymer) and Aquasolve-LG (pH dependent). MicroPET/CT imaging offered valuable *in vivo* data of the behaviour of 3DP devices, using the rat as a model animal. Kollicoat IR and Klucel EF devices disintegrated within 1 to 2h, whilst Aquasolve-LG devices took longer than 7h to disintegrate. Aqualon N7 devices did not disintegrate or release the tracer and gastric emptying was not observed for any of the devices. In addition, this study contributed to the identified inconsistencies regarding the lack of gastric emptying of modified release in *in vivo* studies. Therefore, this pilot study confirmed that 3DP is capable of printing solid dosage forms, however, further work should be employed to fabricate different geometries and smaller devices to successfully empty from the stomach of rats. In summary, the work has highlighted the potential of FDM 3DP in the design of formulations suitable for pre-clinical testing of drugs, and thus, offer advantages towards targeted release and personalised dosing.

References

Albrecht, K., M. Greindl, C. Kremser, C. Wolf, P. Debbage & A. Bernkop-Schnürch (2006) Comparative in vivo mucoadhesion studies of thiomer formulations using magnetic resonance imaging and fluorescence detection. *Journal of Controlled Release,* 115**,** 78-84.

Alomari, M., F. H. Mohamed, A. W. Basit & S. Gaisford (2015) Personalised dosing: Printing a dose of one's own medicine. *Int J Pharm,* 494**,** 568-77.

Anand, S. S., H. Singh & A. K. Dash (2009) Clinical Applications of PET and PET-CT. *Medical Journal, Armed Forces India,* 65**,** 353-358.

Capozzi, M. E., A. Y. Gordon, J. S. Penn & A. Jayagopal (2013) Molecular imaging of retinal disease. *J Ocul Pharmacol Ther,* 29**,** 275-86.

Cunha, L., K. Szigeti, D. Mathe & L. F. Metello (2014) The role of molecular imaging in modern drug development. *Drug Discov Today,* 19**,** 936-48.

Dalziel, J. E., K. Fraser, W. Young, C. M. McKenzie, S. A. Bassett & N. C. Roy (2017) Gastroparesis and lipid metabolism-associated dysbiosis in Wistar-Kyoto rats. *Am J Physiol Gastrointest Liver Physiol,* 313**,** G62-G72.

Dalziel, J. E., W. Young, P. Bercik, N. J. Spencer, L. J. Ryan, K. E. Dunstan, C. M. Lloyd-West, P. K. Gopal, N. W. Haggarty & N. C. Roy (2016) Tracking gastrointestinal transit of solids in aged rats as pharmacological models of chronic dysmotility. *Neurogastroenterol Motil,* 28**,** 1241-51.

Ding, H. & F. Wu (2012) Image Guided Biodistribution and Pharmacokinetic Studies of Theranostics. *Theranostics,* 2**,** 1040-1053.

Fernandez-Ferreiro, A., J. Silva-Rodriguez, F. J. Otero-Espinar, M. Gonzalez-Barcia, M. J. Lamas, A. Ruibal, A. Luaces-Rodriguez, A. Vieites-Prado, T. Sobrino, M. Herranz, L. Garcia-Varela, J. Blanco-Mendez, M. Gil-Martinez, M. Pardo, A. Moscoso, S. Medin-Aguerre, J. Pardo-Montero & P. Aguiar (2017) Positron Emission Tomography for the Development and Characterization of Corneal Permanence of Ophthalmic Pharmaceutical Formulations. *Invest Ophthalmol Vis Sci,* 58**,** 772-780.

Fina, F., A. Goyanes, S. Gaisford & A. W. Basit (2017) Selective laser sintering (SLS) 3D printing of medicines. *International Journal of Pharmaceutics,* 529**,** 285-293.

Goyanes, A., A. B. Buanz, A. W. Basit & S. Gaisford (2014) Fused-filament 3D printing (3DP) for fabrication of tablets. *International Journal of Pharmaceutics,* 476**,** 88-92.

Goyanes, A., A. B. Buanz, G. B. Hatton, S. Gaisford & A. W. Basit (2015a) 3D printing of modified-release aminosalicylate (4-ASA and 5-ASA) tablets. *Eur J Pharm Biopharm,* 89**,** 157-162.

Goyanes, A., H. Chang, D. Sedough, G. B. Hatton, J. Wang, A. Buanz, S. Gaisford & A. Basit (2015b) Fabrication of controlled-release budesonide tablets via desktop (FDM) 3D printing *International Journal of Pharmaceutics,* 496**,** 414-420.

Goyanes, A., F. Fina, A. Martorana, D. Sedough, S. Gaisford & A. W. Basit (2017) Development of modified release 3D printed tablets (printlets) with pharmaceutical

excipients using additive manufacturing. *International Journal of Pharmaceutics,* 527**,** 21-30.

Goyanes, A., M. Kobayashi, R. Martinez-Pacheco, S. Gaisford & A. W. Basit (2016) Fused-filament 3D printing of drug products: Microstructure analysis and drug release characteristics of PVA-based caplets. *Int J Pharm,* 514**,** 290-295.

Goyanes, A., J. Wang, A. Buanz, R. Martinez-Pacheco, R. Telford, S. Gaisford & A. W. Basit (2015c) 3D Printing of Medicines: Engineering Novel Oral Devices with Unique Design and Drug Release Characteristics. *Mol Pharm,* 12**,** 4077-84.

Hatch, M., J. Cornelius, M. Allison, H. Sidhu, A. Peck & R. W. Freel (2006) Oxalobacter sp. reduces urinary oxalate excretion by promoting enteric oxalate secretion. *Kidney International,* 69**,** 691-698.

Hatton, G. B., V. Yadav, A. W. Basit & H. A. Merchant (2015) Animal Farm: Considerations in Animal Gastrointestinal Physiology and Relevance to Drug Delivery in Humans. *J Pharm Sci,* 104**,** 2747-76.

Janssens, S., H. N. de Armas, J. P. Remon & G. Van den Mooter (2007) The use of a new hydrophilic polymer, Kollicoat IR®, in the formulation of solid dispersions of Itraconazole. *European Journal of Pharmaceutical Sciences,* 30**,** 288-294.

Khaled, S. A., J. C. Burley, M. R. Alexander, J. Yang & C. J. Roberts (2015a) 3D printing of five-in-one dose combination polypill with defined immediate and sustained release profiles. *Journal of Controlled Release,* 217**,** 308-14.

Khaled, S. A., J. C. Burley, M. R. Alexander, J. Yang & C. J. Roberts (2015b) 3D printing of tablets containing multiple drugs with defined release profiles. *International Journal of Pharmaceutics,* 494**,** 643-50.

Lameka, K., M. D. Farwell & M. Ichise. 2016. Chapter 11 - Positron Emission Tomography. In *Handbook of Clinical Neurology,* eds. J. C. Masdeu & R. G. González, 209-227. Elsevier.

Liu, F., R. Lizio, C. Meier, H. U. Petereit, P. Blakey & A. W. Basit (2009) A novel concept in enteric coating: a double-coating system providing rapid drug release in the proximal small intestine. *J Control Release,* 133**,** 119-24.

Markl, D., J. A. Zeitler, C. Rasch, M. H. Michaelsen, A. Mullertz, J. Rantanen, T. Rades & J. Botker (2017) Analysis of 3D Prints by X-ray Computed Microtomography and Terahertz Pulsed Imaging. *Pharmaceutical Research,* 34**,** 1037-1052.

McConnell, E. L., A. W. Basit & S. Murdan (2008) Measurements of rat and mouse gastrointestinal pH, fluid and lymphoid tissue, and implications for in-vivo experiments. *J Pharm Pharmacol,* 60**,** 63-70.

Melocchi, A., F. Parietti, G. Loreti, A. Maroni, A. Gazzaniga & L. Zema (2015) 3D printing by fused deposition modeling (FDM) of a swellable/erodible capsular device for oral pulsatile release of drugs. *Journal of Drug Delivery Science and Technology,* 30**,** 360-367.

Melocchi, A., F. Parietti, A. Maroni, A. Foppoli, A. Gazzaniga & L. Zema (2016) Hot-melt extruded filaments based on pharmaceutical grade polymers for 3D printing by fused deposition modeling. *International Journal of Pharmaceutics,* 509**,** 255-263.

Mori, M., Shirai, Y., Uezono, Y., Takahashi, T., Nakamura, Y., Makita, H., Nakanishi, Y. and Imasato, Y. (1989) Influence of Specific Gravity and Food on Movement of Granules in the Gastrointestinal Tract of Rats. *Chemical and Pharmaceuitcal Bulletin,* 37**,** 738-741.

Okwuosa, T. C., B. C. Pereira, B. Arafat, M. Cieszynska, A. Isreb & M. A. Alhnan (2017) Fabricating a Shell-Core Delayed Release Tablet Using Dual FDM 3D Printing for Patient-Centred Therapy. *Pharmaceutical Research,* 34**,** 427-437.

Oveisi, F., S. Gaetani, K. T.-P. Eng & D. Piomelli (2004) Oleoylethanolamide inhibits food intake in free-feeding rats after oral administration. *Pharmacological Research,* 49**,** 461-466.

Rowe, R. C., P. J. Sheskey & M. E. Quinn. 2009. *Handbook of pharmaceutical excipients*. London: Pharmaceutical Press and American Pharmacists Association.

Sanderson, K. (2015) 3D printing: the future of manufacturing medicine? *The Pharmaceutical Journal,* 294**,** No 7865.

Saphier, S., A. Rosner, R. Brandeis & Y. Karton (2010) Gastro intestinal tracking and gastric emptying of solid dosage forms in rats using X-ray imaging. *Int J Pharm,* 388**,** 190-5.

Schiller, C., C. P. Frohlich, T. Giessmann, W. Siegmund, H. Monnikes, N. Hosten & W. Weitschies (2005) Intestinal fluid volumes and transit of dosage forms as assessed by magnetic resonance imaging. *Aliment. Pharmacol. Ther.,* 22**,** 971-979.

Shah, R. B., M. Nutan & M. A. Khan (2004) An Enteric Dual-Controlled Gastrointestinal Therapeutic System of Salmon Calcitonin-I: Preparation, Characterization, and Preclinical Bioavailability in Rats. *Clinical Research and Regulatory Affairs,* 21**,** 81-96.

Shingaki, T., T. Takashima, Y. Wada, M. Tanaka, M. Kataoka, A. Ishii, Y. Shigihara, Y. Sugiyama, S. Yamashita & Y. Watanabe (2012) Imaging of gastrointestinal absorption and biodistribution of an orally administered probe using positron emission tomography in humans. *Clinical Pharmacology and Therapeutics,* 91**,** 653-659.

Sonaje, K., Y.-J. Chen, H.-L. Chen, S.-P. Wey, J.-H. Juang, H.-N. Nguyen, C.-W. Hsu, K.-J. Lin & H.-W. Sung (2010) Enteric-coated capsules filled with freeze-dried chitosan/poly(γ-glutamic acid) nanoparticles for oral insulin delivery. *Biomaterials,* 31**,** 3384-3394.

Tuleu, C., M. K. Khela, D. F. Evans, B. E. Jones, S. Nagata & A. W. Basit (2007) A scintigraphic investigation of the disintegration behaviour of capsules in fasting subjects: a comparison of hypromellose capsules containing carrageenan as a gelling agent and standard gelatin capsules. *European Journal of Pharmaceutical Sciences: Official Journal of the European Federation for Pharmaceutical Sciences,* 30**,** 251-255.

Varum, F. J., G. B. Hatton & A. W. Basit (2013) Food, physiology and drug delivery. *International Journal of Pharmaceutics,* 457**,** 446-60.

Wang, J., A. Goyanes, S. Gaisford & A. W. Basit (2016) Stereolithographic (SLA) 3D printing of oral modified-release dosage forms. *International Journal of Pharmaceutics,* 503**,** 207-212.

Weinstein, D. H., S. deRijke, C. C. Chow, L. Foruraghi, X. Zhao, E. C. Wright, M. Whatley, R. Maass-Moreno, C. C. Chen & S. A. Wank (2013) A new method for determining gastric acid output using a wireless pH-sensing capsule. *Alimentary Pharmacology & Therapeutics,* 37**,** 1198-1209.

Yamashita, S., T. Takashima, M. Kataoka, H. Oh, S. Sakuma, M. Takahashi, N. Suzuki, E. Hayashinaka, Y. Wada, Y. Cui & Y. Watanabe (2011) PET imaging of the gastrointestinal absorption of orally administered drugs in conscious and anesthetized rats. *Journal of Nuclear Medicine: Official Publication, Society of Nuclear Medicine,* 52**,** 249-256.